



# Thermographic Evaluation of Dental Implants Insertion with Different Diameters and Bone Quality on The Primary Stability: A 3D Finite Element Study

Sandipan Mukherjee,<sup>1</sup> Vathsala Patil,<sup>2,\*</sup> Antony V Samrot,<sup>3</sup> Komal Smriti,<sup>2,\*</sup> Shobha J Rodrigues,<sup>1</sup> Swagat Sarkar,<sup>4</sup> Harsh Joshi,<sup>4</sup> Srikanth Gadicherla,<sup>5</sup> Krishna Kumar P<sup>4</sup> and Nithesh Naik<sup>4</sup>

## Abstract

Caries and periodontal disease are the primary causes of tooth loss and extraction. Tooth loss leads to resorption of the alveolar ridge, which can complicate the placement of dental implants. Hybrid prostheses are emerging as effective treatment options for individuals with complete tooth loss, offering a means to restore proper chewing function. Implant dentistry has improved edentulous patients' recovery, with a 10-year success rate of more than 97%. However, the insertion torque, the surface properties of the implants, and the heat created during implant site preparation may all play a role in early implant failure. As a result, monitoring the temperature during the insertion might be critical in predicting the prosthesis success rate. Although various research studies have investigated the thermal consequences of drilling and fixture placement, a comparative analysis of the thermal result of implant insertion of different diameters and bone quality on the primary stability is lacking. The main aim of the research was to assess the heat variations caused by the insertion of a narrow implant using a three-dimensional (3D) finite element analysis. Both narrow and standard implants caused a rise in bone temperature. Furthermore, the narrow implant had a greater thermal effect than standard implants, although it was always lower than the temperature limits of bone necrosis. The findings demonstrated that narrow implants are both thermally and clinically safe.

**Keywords:** Biomechanics; Finite element analysis; Implant; Bone quality; Thermal.

Received: 30 September 2023; Revised: 27 November 2023; Accepted: 29 November 2023.

Article type: Research article.

## 1. Introduction

Despite substantial advancements in diagnosing, preventing, managing, and treating oral diseases, the problem of teeth and supporting tissues lost or damaged due to disease or trauma persists. Across the globe, for people of all ages, a missing tooth can have a range of negative effects on quality of life. These effects encompass challenges in speaking, diminished confidence, and impaired abilities such as chewing,

mastication, and deglutition. Consequently, a decrease in the number of teeth could potentially lead to a lower quality of life.<sup>[1]</sup> Every day, the human tooth experiences thermal variations due to the consumption of foods and beverages of various temperatures. Heat from changes in intra-oral temperature is conducted to the tooth surface, passing through the enamel, dentin, and reaching the pulp. The pulp is protected from abrupt temperature fluctuations because both enamel and dentin have lower thermal conductivity values.<sup>[2]</sup>

Dental implants are recognized as the optimal solution for patients who have partially or fully lost their natural teeth. They provide a stable foundation for artificial replacement teeth and prosthetics, eliminating the instability associated with surface adhesives and removable bridges.<sup>[3,4]</sup>

Dental implants, a common procedure in dentistry, are designed to distribute occlusal loads to the bone and surrounding tissues.<sup>[5]</sup> It's crucial to select the best parameters in terms of mechanical properties and biocompatibility, the

<sup>1</sup> Department of Prosthodontics and Crown & Bridge, Manipal College of Dental Sciences, Mangalore, Manipal Academy of Higher Education, Udupi, Karnataka, 576104, India.

<sup>2</sup> Department of Oral Medicine and Radiology, Manipal College of Dental Sciences, Manipal, Manipal Academy of Higher Education, Udupi, Karnataka, 576104, India.

<sup>3</sup> School of Bioscience, Faculty of Medicine, Bioscience and Nursing, MAHSA University, Jalan SP2, Bandar Saujana Putra, Jenjarom 42610, Selangor, Malaysia

type of implants, and their functional impact. Moreover, mechanical and thermal loads play a significant role in the operation of dental implants and their potential to cause bone damage, making them important considerations for this research. A comprehensive evaluation of dental implant performance can be achieved by modeling and analyzing the effects of mechanical and thermal stress on the implant, considering various implant qualities.<sup>[6-8]</sup>

The mandible and maxilla, both parts of the jaw, contain two types of bone: cortical and cancellous. The main distinction between the two is that cortical bone, is compact, while cancellous bone is a highly porous, mineralized tissue that is enclosed within the cortical bone.<sup>[9]</sup> A titanium implant is commonly used to replace a missing tooth. Dental implants can be either one-piece or two-piece, with a screw connecting the crown and root in both cases. They are considered one of the best options for tooth replacement. However, dental implants can fail for various reasons, including the inability to withstand pressures and torques, and intolerance to high temperatures.<sup>[10]</sup> Some studies have investigated stress shielding and remodeling to assess implant function and potential flaws in the bone-implant interface to evaluate stress distribution patterns.<sup>[11]</sup>

The failure of dental implants can lead to undesirable complications. For an implant to be successful, it needs stability, resistance to applied forces, and minimal bone strain around the implant. This study aims to perform a numerical and three-dimensional analysis of jaws with implants under mechanical, thermal, and thermomechanical loading using the finite element method. However, many studies have focused more on the durability of the implants rather than the bone-implant complex.<sup>[12]</sup> In this context, the SimSolid program is used to simulate dental implants with a titanium root, mandibular bone, and mucosa under dynamic and thermal pressure. The findings of this research suggest that high-temperature tolerance can develop while piercing the mandibular bone and/or consuming hot liquids.

By creating a model of the set of implants and mandibular bone, and taking into account mechanical and thermal loads, we can compute the stress distribution, strain, and

displacement in both the implant and mandibular bone. This allows us to examine the influence of various factors on these parameters. The traditional method for quantitatively assessing stresses on the implant and its surrounding bone has been through three-dimensional (3-D) finite element analysis (FEA).<sup>[13,14]</sup> Finite element analysis (FEA) was selected as the preferred method to examine the effects of static and dynamic loads on the stress distribution for an implant-supported fixed partial denture and the supporting bone tissue, as well as the fatigue behavior of the implant complex. The goal of this study was to calculate the optimal lifespan for an Osseo-integrated implant. In conclusion, the finite element method enables the simulation of real conditions of biomechanical structures with a satisfactory level of approximation.<sup>[15]</sup>

The present study provides insight into how the mandibular bone responds to the thermal conditions that occur around dental implants. Increased temperatures around the implant have been known to cause necrosis of the bone. The effect of increased temperatures around the implant during osteotomy preparation has been studied extensively. However, literature is scarce regarding the effect of temperature post-insertion and depth of insertion of different diameters (narrow and standard diameters) of implants. This study is an attempt to understand the same.

## 2. Materials and methods

### 2.1 Construction of the 3D model

The construction of the 3D model was initiated with a completely edentulous mandible generated from CT scan data in DICOM format, measuring 31 mm in height and 80 mm in length. While the model displayed an overall height of 31 mm, a significant bone loss was evident in the symphysis region, resulting in a reduced height of only 28 mm. MIMICS® v14.1 software facilitated initial data processing, converting it into a 3D model. Further refinement and repair were performed using ANSYS SpaceClaim software (V22.1), addressing concerns like curves, gaps, missing faces, and extraneous edges. The model was meticulously divided into two parts: an outer cortical bone layer and an inner volume of trabecular bone, enabling detailed characterization.

To simulate and analyze the response of the assembled model under varying conditions, the model was exported to SimSolid®. This software, renowned for its proficiency in structural analysis, generated high-order functions automatically based on the geometry of the imported model. The simulation process was executed leveraging these automatically generated functions, bypassing the need for manual mesh generation. This approach streamlined and expedited the analysis while preserving accuracy and reliability in predicting the model's behavior under different loading scenarios.

SimSolid® proves to be instrumental in providing an efficient and accurate means to investigate the structural

---

<sup>4</sup> Department of Mechanical and Industrial Engineering, Manipal Institute of Technology, Manipal Academy of Higher Education, Manipal 576104, Karnataka, India.

<sup>5</sup> Department of Department of Oral and Maxillofacial Surgery, Manipal College of Dental Sciences, Manipal, Manipal Academy of Higher Education, Udupi, Karnataka, 576104, India.

\*Email: [vathsala.mcodes@manipal.edu](mailto:vathsala.mcodes@manipal.edu) (V. Patil);  
[komal.smriti@manipal.edu](mailto:komal.smriti@manipal.edu) (K. Smiriti)

integrity, stress distribution, and mechanical responses. The software's capability to handle complex geometries and perform analyses without mesh generation significantly expedites the assessment process, enabling a comprehensive understanding of the model's mechanical behavior.

## 2.2 Material properties

This study, which was approved by the institutional ethics committee (IEC No. 23074/2023), adhered to ethical standards and was conducted in accordance with the ethical guidelines laid down by the Declaration of Helsinki (2013). Titanium, with a modulus of elasticity of 110 GPa and a Poisson's ratio of 0.3, is considered the most preferred dental implant material due to its biocompatibility and suitability for most patients. Titanium metal implants promote proper bone growth when placed in contact with the bone and left undisturbed. The bone grows adjacent to them, leading to a lasting connection to the bone. According to Carl Misch *et al.*, the bone in the maxilla and mandible can be classified according to its quality as D1, D2, D3, and D4 types, considering three different characteristics of the bone tissue: location, composition, and density. The impact of bone quality on the implant is reflected during the implant placement procedure, with implant design and surface treatment being adjusted to match the bone quality. For this study, we consider three types of bones - D1, D2, and D3 - with a layer of mucosa resting on top. D1 bone is primarily composed of cortical bone mass, which is predominantly found in the anterior mandible. D1 bone is indicated by a Hounsfield unit reading of 1250 or higher. This type of bone has the highest bone-to-implant contact (BIC) and provides superior initial implant stability. Due to its density, this type of bone has fewer intrinsic blood vessels and heavily relies on the periosteum for nutrition and blood delivery<sup>13</sup>.

On the other hand, D2 bone consists of a thick cortical crestal layer and coarse trabecular bone beneath the cortical bone. This type of bone is typically present in both the anterior and posterior regions of the mandible. A Hounsfield reading of 850 to 1250 units indicates D2 bone.

Due to its coarse structure, this type of bone has a high BIC ratio and abundant intrinsic vascularization. In terms of drill diameter sequence, the drill technique for D2 bone is slightly less demanding; fewer drills may be required to achieve final osteotomy dimensions. Drill speed, applied force, pumping motion, and irrigation with pre-cooled, sterile saline solution are all similar to those used in D1 bone. Table 1 discusses the material properties of the bone type and implant used in the study. D3 bone consists of a porous crestal layer of cortical bone and fine trabecular bone beneath the cortical bone. This type of bone is primarily found in the anterior and posterior maxilla, but also the posterior mandible. A Hounsfield reading between 350 and 850 units indicates D3 bone. The implant stability increases with the elastic modulus. However, since D1 is purely cortical, it requires additional care during osteotomy preparation. Inadequate cooling during the

procedure can lead to excessive heat generation, which can cause bone necrosis and implant failure. The best implant stability is observed in D1, D2, and D3 types of bones.

**Table 1.** Properties of Titanium implant, cortical bone D1, trabecular bones D2 and D3, and mucosa used in the study.

Material	Young's modulus (GPa)	Poisson's Ratio	Thermal Conductivity (W/mK)	Material Density (Kg/m <sup>3</sup> )
Titanium Implant & Abutment	116	0.4	0.17	4500
Cortical Bone (D1)	14.8	0.3	0.6	2000
Trabecular bone (D2)	0.55	0.3	0.2	219
Trabecular bone (D3)	0.16	0.3	0.2	219
Mucosa	0.005	0.4	0.34	1200

## 2.3 Loading and boundary conditions using SimSolid®

To ensure accurate alignment and orientation of prosthetic parts, ANSYS SpaceClaim software employed the 'align' command, meticulously aligning axes in both anterior and posterior regions. The 'align' command was further utilized to align the framework's bottom surface precisely with the abutment surface, ensuring a snug fit and maximum stability. Creating a threaded hole involved Boolean operations on mandibular and mucosal 3D models, utilizing the 'intersect' operation to sculpt the threaded hole geometry by intersecting implant threads with these surfaces.

Upon assembly, the model transitioned into a Parasolid file format and was imported into SimSolid® (2022, Altair, Troy, MI, USA) for analysis. The software autonomously generated high-order functions based on the model's geometry, facilitating simulations without manual mesh generation. This streamlined the analysis process, ensuring efficiency and accuracy in evaluating the constructed 3D model's behavior under various loading conditions.

## 2.4 Mechanical aspects and equations

### 2.4.1 Stress and strain analysis

The mechanical performance of dental implants under loading conditions is crucial for assessing their stability and longevity. The relationship between stress ( $\sigma$ ) and strain ( $\epsilon$ ) is fundamental in understanding material behavior.

### 2.4.2 Stress calculation

Stress is computed using equation (1), while strain is calculated utilizing equation (2), as detailed in the literature Ref. [10-12].

$$\sigma = \frac{F}{A} \quad (1)$$

where F represents the applied force and A is the cross-sectional area of the implant.

**2.4.3 Strain calculation**

$$\epsilon = \frac{L}{\delta} \tag{2}$$

where  $\delta$  denotes the displacement and  $L$  is the original length of the implant.

**2.4.4 Hooke's law for elasticity**

Hooke's Law characterizes the relationship between stress and strain in linearly elastic materials as shown in [equation \(3\)](#),

$$\sigma = E \cdot \epsilon \tag{3}$$

here,  $E$  signifies Young's Modulus, describing the material's stiffness and its resistance to deformation.

**2.4.5 Implant Stability Quotient (ISQ)**

The Implant Stability Quotient (ISQ) is a critical measure obtained through resonance frequency analysis systems,

$$ISQ = \frac{f_{max} - f_{min}}{f_{measured} - f_{min}} \times 100 \tag{4}$$

In this [equation \(4\)](#), measured  $f_{measured}$  represents the measured frequency,  $f_{max}$  is the maximum frequency, and  $f_{min}$  is the minimum frequency obtained during resonance frequency analysis.

**2.5 Thermal analysis**

Thermal analysis is performed on the Implant System at various depths of insertion. This process involves simulating and analyzing the heat transfer and thermal behavior of a design under different thermal loading conditions. The temperature range considered in this study, from 5 °C to 55 °C, is significant as it represents the provocation temperatures, with 5 °C for cold provocation and 55 °C for hot provocation. This range helps to understand how the implant system responds to temperature changes that mimic real-world conditions.

**2.5.1 Heat transfer equations**

Understanding the heat transfer,  $Q$  given in [equation \(5\)](#) within the implant system is crucial for assessing its response to varying temperatures,

$$Q = -kA \frac{dx}{dT} \tag{5}$$

Here,  $Q$  represents the rate of heat transfer,  $k$  is the thermal conductivity,  $A$  is the cross-sectional area,  $dT$  represents the temperature gradient, and  $dx$  is the distance over which the gradient occurs. These above equations enable the quantitative assessment of mechanical stresses, strains, and thermal behavior within dental implant materials, providing insights into their structural integrity and response to environmental conditions.

**3. Results**

The results of the temperature variation were observed in the implant-mandibular bone assembly for 12 cases of –different bone types (D1, D2, and D3), implant diameters (3.5 mm and 4.5 mm), and the depth of insertion of the implant (0, 0.5 and 1 mm). The results of the analysis are shown in [Tables 2, 3, and 4](#) for various temperatures at 5°, 20°, 35° and 50° temperatures on the surface of the abutment for 3.5 mm and 4.5 mm implants at three depths of insertions – 0 mm, on 0.5 mm and 1 mm on the different bone types.

In the study conducted to assess the thermal behavior of dental implants within D1 bone, [Figs. 1A and 1B](#) depict detailed observations regarding the maximum temperatures at different insertion depths for 3.5 mm and 4.5 mm implants, respectively. These figures serve as critical visual representations of the thermal response of implants within high-density cortical bone.

[Table 2](#) encapsulates a comprehensive summary of the temperature observations across various scenarios and implant sizes within the D1 bone. Notably, it delineates distinct thermal behaviors exhibited by the 3.5 mm and 4.5 mm implants at different insertion depths and temperature ranges. The findings unveiled distinctive patterns in temperature

**Table 2.** Thermal response of 3.5mm and 4.5mm Implants in D1 Bone at different depths of insertion.

Depth of Insertion (mm)	Temperature of the Source (°C)	3.5mm			4.5mm			
		Maximum Temperature At (°C)			Maximum Temperature At (°C)			
		Bone	Implant	Entire System	Bone	Implant	Entire System	
D1	0	5	16.9	14.8	18.0	15.7	13.2	17.1
		20	23.0	22.4	23.3	22.7	22.0	23.1
		35	32.3	35.0	35.0	32.8	35.0	35.0
	0.5	5	43.3	50.0	50.0	44.4	50.0	50.0
		20	16.6	14.2	17.8	15.3	12.9	16.7
		35	22.9	22.3	23.2	22.6	21.8	23.0
	1	5	32.6	35.0	35.0	33.1	35.0	35.0
		20	44.1	50.0	50.0	45.1	50.0	50.0
		35	16.4	14.0	17.6	15.0	12.6	16.5
		5	22.9	22.2	23.2	22.6	21.9	22.9
		20	32.8	35.0	35.0	33.2	35.0	35.0
		35	44.6	50.0	50.0	45.5	50.0	50.0

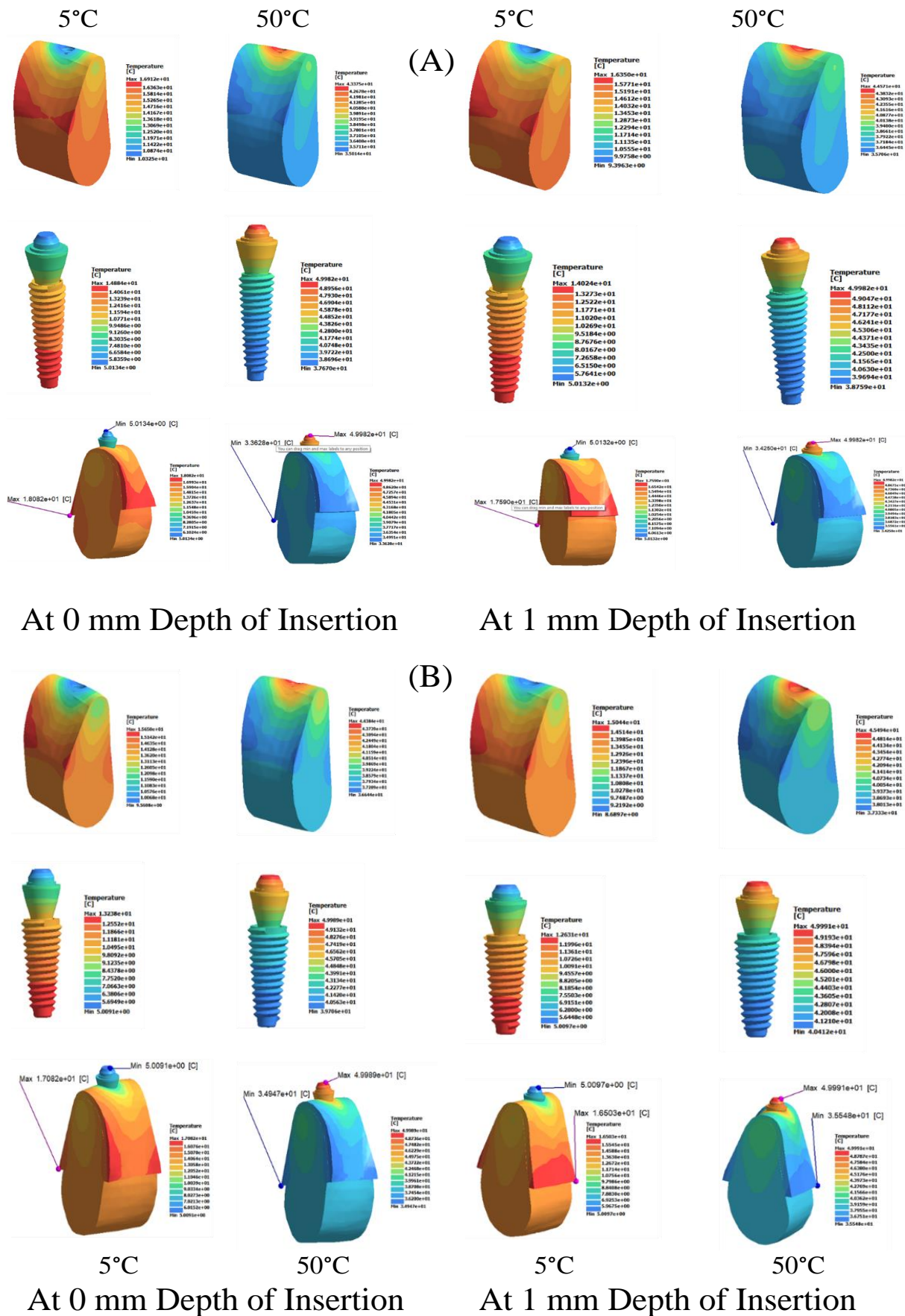


**Fig. 1** A: Thermal stress distribution in 3.5mm implant and D1 bone type system, B: Thermal stress distribution in 4.5mm implant and D1 bone type system.

distribution concerning implant size, depth of insertion, and environmental temperature. For both 3.5 mm and 4.5 mm implants, the maximum temperatures at the bone level consistently manifested at a 1 mm depth of insertion across all temperature ranges. However, beyond 20 °C, the maximum temperatures remained relatively constant at the implant and system levels for 35 °C and 50 °C, irrespective of insertion depth.

Comparative analyses between the two implant sizes revealed intriguing nuances. At lower temperatures (5 °C and 20 °C), the 3.5 mm implant consistently exhibited higher temperatures at the bone level across various depths of insertion when contrasted with the 4.5 mm implant. This disparity might be attributed to the smaller implant's potentially higher heat retention capacity due to its relatively smaller surface area in contact with the bone. Conversely, at elevated temperatures (35 °C and 50 °C), the 4.5 mm implant consistently showcased higher temperatures at the bone level across all insertion depths compared to its 3.5 mm counterpart. This shift in thermal behavior possibly indicates the larger implant's tendency to accumulate more heat, affecting the surrounding bone tissue differently. The observations emphasize the intricate interplay between implant dimensions, depth of insertion, and environmental temperature on the thermal responses within high-density cortical bone. Such insights are crucial for optimizing implant design, insertion techniques, and temperature management protocols to mitigate potential risks such as bone necrosis and implant failure associated with excessive heat generation during the placement procedure.

These findings align with previous studies<sup>[7-12]</sup> indicating the influence of implant geometry on thermal characteristics within bone tissues. They contribute substantially to the understanding of implant-bone interactions, serving as a foundational reference for further research aimed at refining implant materials and insertion methodologies to enhance patient outcomes and minimize thermal-related complications in dental implantology.

Table 2 represents a detailed assessment of how 3.5 mm and 4.5 mm dental implants respond to varied source temperatures (5 °C, 20 °C, 35°C, and 50°C) across different depths of insertion within the high-density D1 bone. It meticulously documents the maximum temperatures recorded at critical levels: bone, implant, and the entire system, offering insights into the implants' thermal behavior. At lower temperatures (5 °C and 20 °C), the 3.5 mm implant tends to exhibit marginally higher temperatures at the bone level compared to the 4.5 mm counterpart across various insertion depths. However, as temperatures escalate to 35 °C and 50 °C, a notable shift occurs. The 4.5 mm implant consistently showcases higher temperatures at the bone level across all insertion depths, surpassing the 3.5 mm implant.

These patterns highlight the intricate thermal dynamics between different implant sizes and bone environments, suggesting potential implications for clinical approaches and implant designs. Understanding these nuances becomes pivotal in refining strategies to manage and alleviate thermal effects during dental implant procedures for optimal patient outcomes.

Similar results as D1 bone was observed in D2 and D3 concerning temperature variations at bone levels, implants, and the entire system irrespective of the implant diameters of 3.5mm and 4.5 mm for all temperatures and all depths of insertions. Table 3 presents intricate insights into the thermal responses of 3.5mm and 4.5 mm dental implants within D2 bone across varying insertion depths and source temperatures. Figs. 2A and 2B visually represent these outcomes, showcasing the maximum temperatures observed at different depths of insertion for each implant size. At 5 °C and 20 °C, the 3.5mm implant consistently registered slightly lower maximum temperatures at the bone level compared to the 4.5mm implant, implying potential disparities in heat dispersion capabilities between the two sizes. Remarkably, at 35 °C and 50 °C, pivotal shifts unfolded. The larger 4.5mm implant consistently displayed higher maximum temperatures at the bone level across all depths of insertion, surpassing

**Table 3.** Thermal response of 3.5 mm and 4.5 mm implants in D2 bone at different depths of insertion.

Depth of Insertion (mm)	Temperature of the Source (°C)	3.5 mm			4.5 mm		
		Maximum Temperature At (°C)			Maximum Temperature At (°C)		
		Bone	Implant	Entire System	Bone	Implant	Entire System
0	5	17.5	14.2	18.8	16.9	13.2	18.1
	20	23.2	22.3	23.5	23.0	22.0	23.3
	35	32.5	35.0	35.0	32.8	35.0	35.0
	50	43.9	50.0	50.0	44.5	50.0	50.0
D2 0.5	5	17.2	13.8	18.5	16.3	12.9	17.3
	20	23.1	22.2	23.4	22.9	21.9	23.1
	35	32.8	35.0	35.0	33.1	35.0	35.0
	50	44.6	50.0	50.0	45.2	50.0	50.0
1	5	17.0	13.9	18.1	16.0	12.6	17.1
	20	23.1	22.2	23.4	22.8	21.9	23.3
	35	32.9	35.0	35.0	33.1	35.0	35.0
	50	44.7	50.0	50.0	45.4	50.0	50.0

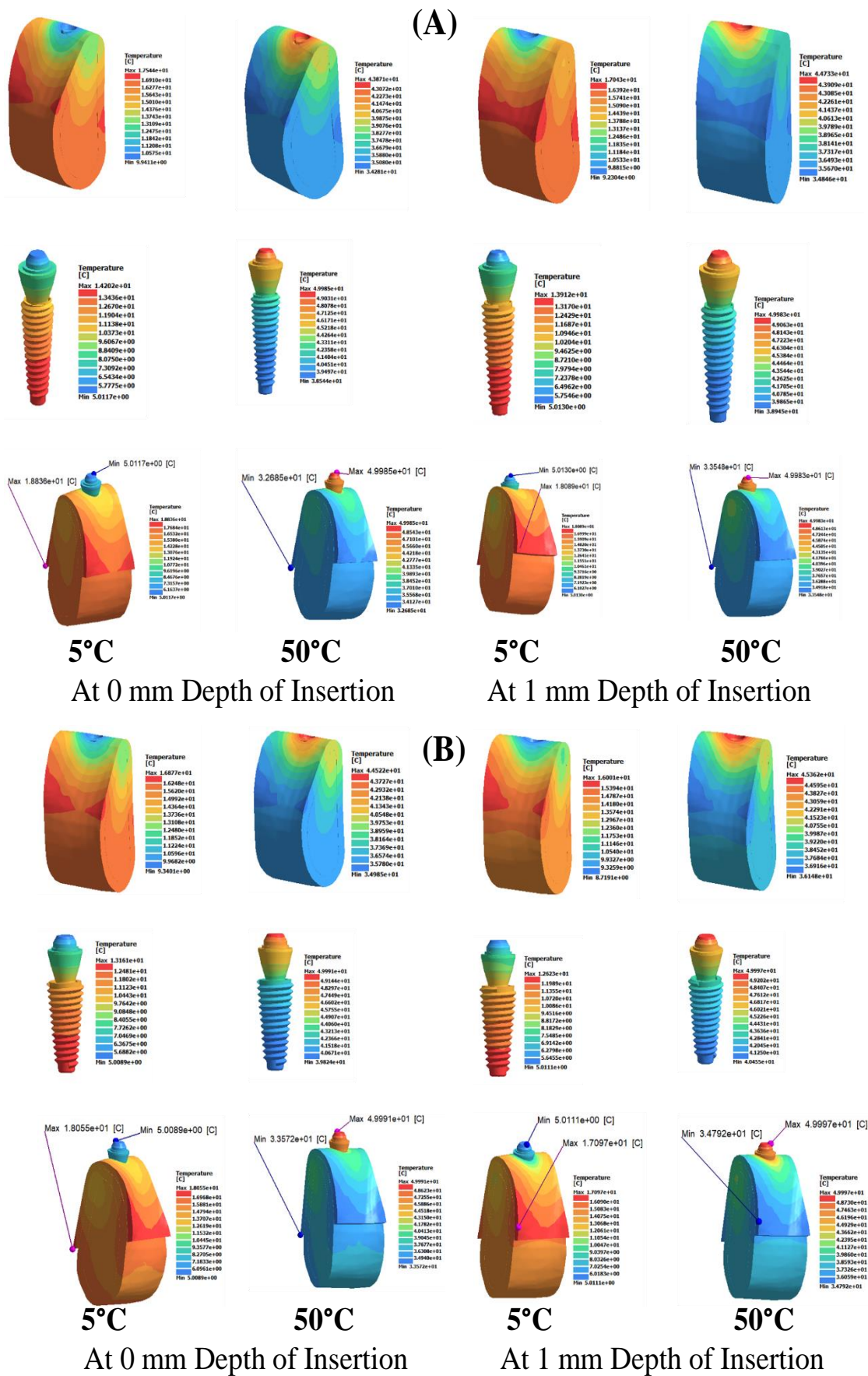


**Fig. 2** A: Thermal stress distribution in 3.5 mm implant and D2 bone type system; B: Thermal stress distribution in 4.5 mm implant and D2 bone type system.

the 3.5mm implant's thermal readings. For instance, at 50 °C, the 4.5 mm implant recorded a maximum bone temperature of 45.4 °C, while the 3.5 mm implant reached 44.7°C, indicating a substantial difference in heat retention between the two sizes. These values underscore the 4.5 mm implant's tendency to retain more heat within the bone tissue at elevated temperatures. Such nuanced observations stress the critical influence of implant size and insertion depth on thermal behaviors within D2 bone, mandating tailored approaches in clinical practices.

Table 4, discusses the thermal responses of 3.5 mm and 4.5 mm dental implants within D3 bone across various insertion depths and source temperatures. At 5 °C, both implants showed distinct differences in bone temperature, with the 3.5 mm implant recording a minimum of 13.1 °C while the 4.5 mm implant reached 14.6 °C, showcasing their varied heat dissipation capacities. As temperatures surged to 50 °C, a significant trend emerged. The larger 4.5 mm implant consistently exhibited higher maximum temperatures at the bone level across all depths of insertion compared to the 3.5 mm implant. For instance, at a depth of 1mm and 50 °C source temperature, the 4.5 mm implant recorded a maximum bone temperature of 45.6 °C, while the 3.5 mm implant reached 43.0 °C, underscoring a notable difference in heat retention between the two sizes. These values exemplify the 4.5 mm implant's propensity to retain more heat within the bone tissue under elevated temperatures. These findings underscore the pivotal influence of implant size and insertion depth on thermal behaviors within the D3 bone, bearing significant implications for clinical approaches.

Understanding these nuances becomes crucial in devising tailored strategies to mitigate potential thermal complications during dental implant procedures. Figs. 3A and 3B visually depict these outcomes, offering a concise visualization of the maximum temperatures observed at different insertion depths for each implant size within the D3 bone. Such comprehensive data serve as foundational insights for optimizing implant designs and insertion techniques to ensure safer and more

efficacious dental implant procedures.

#### 4. Discussion

A study conducted by Poovarodom *et al.*<sup>[12]</sup> aimed to assess the impact of sub-crestal implant placement depth on bone remodeling. This was done using time-dependent finite element analysis (FEA) with a bone-remodeling algorithm over 12 months on cortical and cancellous bone. The study examined the biomechanical responses in both the bone and the implant. The von Mises stresses were evaluated at depths of 0, 0.5, 1.0, 1.5, 2.0, 2.5, and 3.0 mm. The results indicated that the deeper the implant placement, the greater the stress generated, regardless of the type of bone. Placement beyond 1.5 mm resulted in maximum stress generation. Therefore, this current study considered implant placement depths of 0, 0.5, and 1 mm.

Thus, this study considered various clinically feasible depths of insertions and observed the effects of various temperatures at the bone and implant levels and the entire system with 3.5 mm (narrow diameter) and 4.5 (standard diameter) of implants on different bone types. The results obtained showed a correlation of the bone type with the temperature and with depth of insertion. For both the narrow diameter and standard diameter the temperatures increased with an increase in depth of insertion irrespective of the bone type and as the bone type changed from cortical to cancellous the temperatures increased from D1 to D3 at various depths of insertion for the implant diameters.

Wong *et al.*<sup>[16]</sup> proposed that a temperature of 47 °C could develop at a distance of 3 to 4.5 mm along the implant when the implant head is heated to 60 °C to 70 °C. The temperatures in this study were well within the limits suggested by Wong *et al.* for all bone types. The temperatures at the bone and implant levels at different depths of insertion, different bone types, and different diameters of implants have not been studied extensively, as per the authors' knowledge. This current study demonstrates a direct correlation between the diameter of the implant with different bone types and temperatures at bone

**Table 4.** Thermal response of 3.5 mm and 4.5 mm implants in D3 bone at different depths of insertion.

Depth of Insertion (mm)	Temperature of the Source (°C)	3.5 mm			4.5 mm		
		Maximum Temperature At (°C) Bone	Maximum Temperature At (°C) Implant	Maximum Temperature At (°C) Entire System	Maximum Temperature At (°C) Bone	Maximum Temperature At (°C) Implant	Maximum Temperature At (°C) Entire System
0	5	18.1	14.6	19.3	17.4	13.1	18.3
	20	23.3	22.4	22.6	23.2	22.0	23.4
	35	32.1	35.0	35.0	32.8	35.0	35.0
	50	42.6	50.0	50.0	44.6	50.0	50.0
D3 0.5	5	17.3	13.1	18.3	17.7	12.8	17.3
	20	23.1	22.0	23.3	23.1	21.9	23.1
	35	32.5	35.0	35.0	33.1	35.0	35.0
1	50	43.8	50.0	50.0	45.2	50.0	50.0
	5	18.1	14.1	19.0	17.0	12.7	17.9
	20	23.3	22.2	23.6	23.0	21.9	23.3
	35	32.2	35.0	35.0	33.2	35.0	35.0
	50	43.0	50.0	50.0	45.6	50.0	50.0

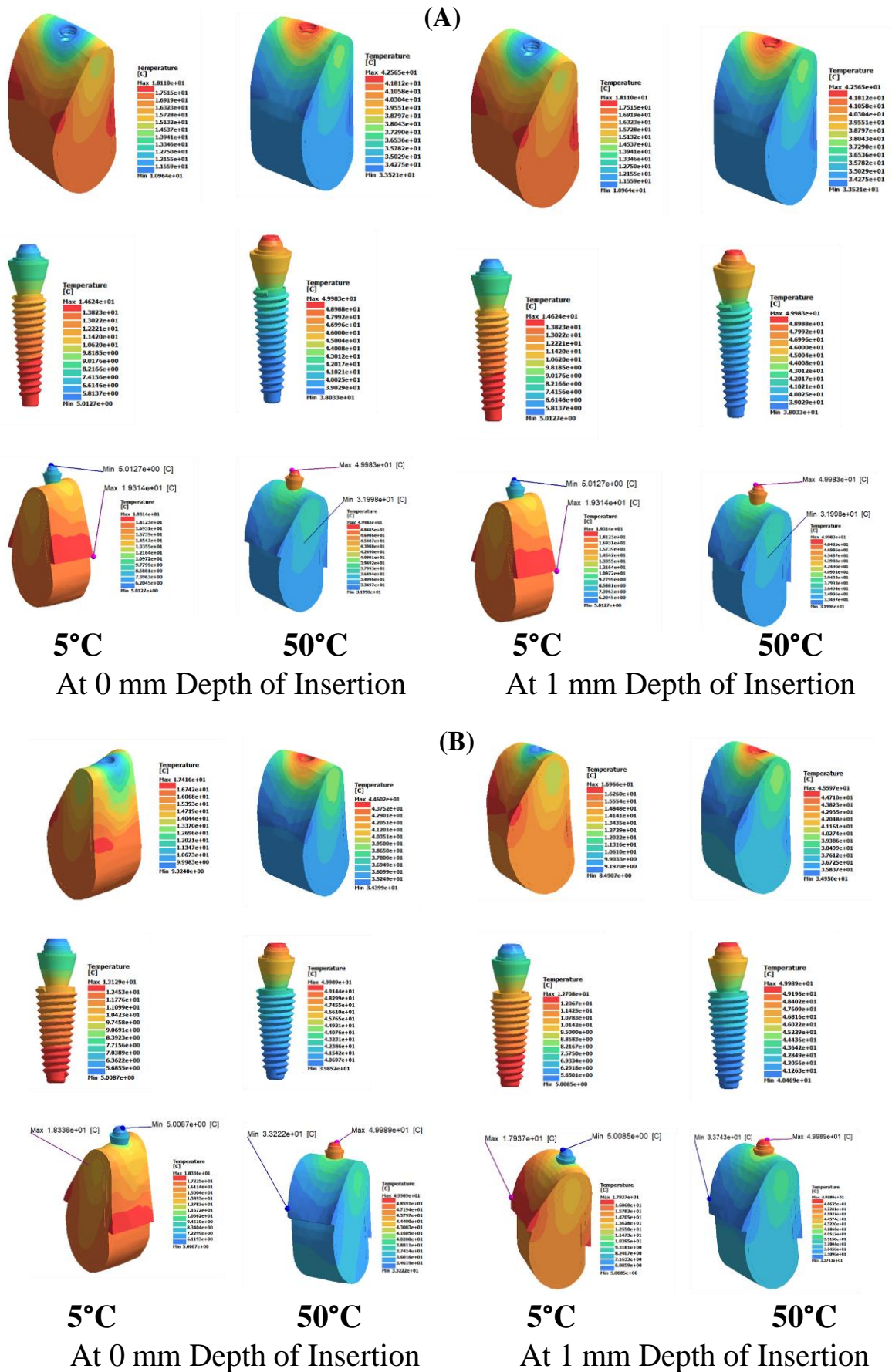


**Fig. 3** A: Thermal stress distribution in 3.5mm implant and D3 bone type system, B: Thermal stress distribution in 4.5mm implant and D3 bone type system.

and implant levels individually and the entire system.

The research indicates that for a 3.5 mm implant, the highest temperature at the bone level was observed at a 1mm depth of insertion across all temperature ranges. With an increase in temperature, the maximum temperatures rose to 35 °C at the bone level and then stabilized at the implant level. This suggests that an increase in the depth of insertion leads to an increase in the maximum temperature. The same pattern was observed for the 4.5 mm implant. This could be due to an increase in bone density as the depth of insertion increases, regardless of the type of bone, leading to an increase in maximum temperature. Past research has shown that denser masses have higher thermal conductivity. Another possible explanation is that the implant disperses the heat to the bone, which could increase bone temperature.

The study also found that implants with a wider diameter could result in less heat transfer, leading to a smaller rise in temperatures in the surrounding bone. This was consistent across all types of bone, suggesting that a larger surface area allows for better heat distribution and thus a smaller rise in temperature compared to implants with a narrow diameter. Therefore, it is crucial to load the implant as soon as possible, as it has been suggested that implants without crowns can lead to more heat transfer. However, more research is needed to understand the relationship between different types of crowns, different implant materials, the duration of contact with hot substances, and depths of insertion and their effects on temperatures at the bone level on different types of bones.

## 5. Conclusion

This study employed 3D finite element analysis to examine how the temperature around a dental implant changed when it was narrow versus when it was standard. The prevalence of dental caries and periodontal disease means that many teeth are still being lost or extracted, highlighting the need for reliable tooth replacement options. Complete tooth loss patients now have viable treatment alternatives in the form of hybrid prostheses, which can restore not only their oral health but also their standard of living. The past decade has seen incredible advancements in implant dentistry, which now has an astounding success rate of over 97% after 10 years. Early implant failure can be caused by a variety of variables, including but not limited to insertion torque, implant surface characteristics, and heat created during site preparation. The heat effect during implant insertion is a very important facet of this procedure. Our study showed that the temperature of the bone rises during the placement of both narrow and regular implants. Although the temperatures were significantly below the threshold for bone necrosis, thin implants did show a somewhat larger thermal effect than their conventional counterparts. This data demonstrates that patients can feel secure choosing thin implants, despite the possibility of heat consequences. When working with patients who have anatomical limitations, dentists and oral surgeons can feel comfortable recommending narrow implants. These implants

can be used in patients with limited bone quality or quantity without worrying too much about the development of thermal problems. Further, our findings highlight the need for more investigation into implant dentistry so that we can learn more about the complex aspects that influence implant success. Dental restorations have come a long way in terms of improving patients' oral health and overall well-being, and they will continue to do so as science and practice evolve.

## 6. Limitations and future scope of work

Identification of the potential disparity between simulated and real-life outcomes is pivotal, urging cautious interpretation of this study's results. Moreover, while assuming material properties' constancy serves modeling simplicity, it overlooks the inherent fluctuations in these properties within clinical contexts. To address these limitations, forthcoming investigations could delve into comprehensive thermographic evaluations. Exploring diverse implant materials and their thermal responses across varying insertion depths would enrich our understanding beyond the confines of titanium implants. Extending these assessments to include implants restored with diverse crown materials could illuminate their thermal interplay within different insertion depths. These future trajectories stand as crucial stepping stones, promising a deeper comprehension of thermal dynamics in dental implantology and paving the way for adaptable and refined clinical methodologies.

## Conflict of Interest

There is no conflict of interest.

## Supporting Information

Not applicable.

## References

- [1] P. Linsuwanont, A. Versluis, J. E. Palamara, H. H. Messer, Thermal stimulation causes tooth deformation: a possible alternative to the hydrodynamic theory? *Archives of Oral Biology*, 2008, **53**, 261-272, doi: 10.1016/j.archoralbio.2007.10.006.
- [2] R. Scheid, J. B. Woelfel, *Woelfel's dental anatomy: its relevance to dentistry*, 7th ed.; Lippincote Williams & Wilkins: Baltimore, MD, USA, 2007.
- [3] G. M. Scotttcecci, C. Misch, K. Benner, *Implants and restorative dentistry*, Martin Dunitz: London, UK, 2001.
- [4] C. Santiuste, M. Rodríguez-Millán, E. Giner, H. Miguélez, The influence of anisotropy in numerical modeling of orthogonal cutting of cortical bone, *Composite Structures*, 2014, **116**, 423-431, doi: 10.1016/j.compstruct.2014.05.031.
- [5] T. Achour, A. Merdji, B. Bachir Bouiadjra, B. Serier, N. Djebbar, Stress distribution in dental implant with elastomeric stress barrier, *Materials & Design*, 2011, **32**, 282-290, doi: 10.1016/j.matdes.2010.05.053.
- [6] J. J. Schwiedrzik, U. Wolfram, P. K. Zysset, A generalized

- anisotropic quadric yield criterion and its application to bone tissue at multiple length scales, *Biomechanics and Modeling in Mechanobiology*, 2013, **12**, 1155-1168, doi: 10.1007/s10237-013-0472-5.
- [7] A. Merdji, B. Bachir Bouiadjra, T. Achour, B. Serier, B. Ould Chikh, Z. O. Feng, Stress analysis in dental prosthesis, *Computational Materials Science*, 2010, **49**, 126-133, doi: 10.1016/j.commatsci.2010.04.035.
- [8] M. O. Hussein, Stress-strain distribution at bone-implant interface of two splinted overdenture systems using 3D finite element analysis, *The Journal of Advanced Prosthodontics*, 2013, **5**, 333, doi: 10.4047/jap.2013.5.3.333.
- [9] S. M. Al-Zubaidi, A. A. Madfa, A. A. Mufadhal, M. A. Aldawla, O. S. Hameed, X.-G. Yue, Improvements in clinical durability from functional biomimetic metallic dental implants, *Frontiers in Materials*, 2020, **7**, 106, doi: 10.3389/fmats.2020.00106.
- [10] S. Yokoyama, N. Wakabayashi, M. Shiota, T. Ohyama, The influence of implant location and length on stress distribution for three-unit implant-supported posterior cantilever fixed partial dentures, *The Journal of Prosthetic Dentistry*, 2004, **91**, 234-240, doi: 10.1016/j.prosdent.2003.12.017.
- [11] N. Okumura, R. Stegaroiu, E. Kitamura, K. Kurokawa, S. Nomura, Influence of maxillary cortical bone thickness, implant design and implant diameter on stress around implants: a three-dimensional finite element analysis, *Journal of Prosthodontic Research*, 2010, **54**, 133-142, doi: 10.1016/j.jpor.2009.12.004.
- [12] P. Poovarodom, C. Rungsiyakull, J. Suriyawanakul, Q. Li, K. Sasaki, N. Yoda, P. Rungsiyakull, Effect of implant placement depth on bone remodeling on implant-supported single zirconia abutment crown: a 3D finite element study, *Journal of Prosthodontic Research*, 2023, **67**, 278-287, doi: 10.2186/jpr.jpr\_d\_22\_00054.
- [13] L.-J. Chen, X.-P. Guo, Y.-M. Li, T.-B. Li, Finite element analysis for interfacial stress and fatigue behaviors of biomimetic titanium implant under static and dynamic loading conditions, *Journal of Central South University(Medical Science)*, 2010, **35**, 662-672, doi: 10.3969/j.issn.1672-7347.2010.07.004.
- [14] I. Alkan, A. Sertgöz, B. Ekici, Influence of occlusal forces on stress distribution in preloaded dental implant screws, *The Journal of Prosthetic Dentistry*, 2004, **91**, 319-325, doi: 10.1016/j.prosdent.2004.01.016.
- [15] F. Wang, H. P. Lee, C. Lu, Thermal-mechanical study of functionally graded dental implants with the finite element method, *Journal of Biomedical Materials Research Part A*, 2007, **80A**, 146-158, doi: 10.1002/jbm.a.30855.
- [16] Kevan, Wong, A model of temperature transients in dental implants, *Biomaterials*, 2001, **22**, 2795-2797, doi: 10.1016/S0142-9612(01)00023-0.
- Publisher's Note:** Engineered Science Publisher remains neutral with regard to jurisdictional claims in published maps and institutional affiliations.